Unsupervised Pattern Recognition of 3D ^{1}H-MRS Prostate Data: A Visual Aid in Tumour Localisation

S. Dodds[1], G. Postma[1], L. Buydens[1], T. Scheenen[2], J. Barentsz[2], T. Roelofs[2], A. Heerschap[2]

[1]Analytical Chemistry, Radboud University Nijmegen, Nijmegen, Netherlands, [2]Radiology, University Medical Center Nijmegen, Nijmegen, Netherlands

Introduction

Magnetic resonance imaging (MRI) and, increasingly, magnetic resonance spectroscopy (MRS) are used for non-invasive localisation and diagnosis of tumours (1). Unsupervised pattern recognition of 2D MRS data in the brain has proliferated strongly over the last few years (2,3), largely via the Europe-wide INTERPRET project (4). Recently, 3D MRS has been introduced for prostate cancer diagnosis. The spectra obtained from the prostate contain relatively little information - for each voxel only three peaks are identifiable, representing choline (Cho), creatine (Cr) and citrate (Cit). One possible method for discriminating tumorous voxels is based on a ratio term derived from the integral values for the three detectable metabolites (5). This work presents an alternative method, using unsupervised pattern recognition of this integral data. With this technique, it is possible to automatically eliminate many voxels which lie outside of the prostate. It is also possible to display the final clustering results in a manner which may serve as a useful visual aid for tumour localisation.

Materials and Methods

Data from around 20 male patients with proven prostate cancer and treated with a radical prostatectomy were used in this study. The patients gave their informed consent prior to the MR exam. They did not have contra-indications to the MR exam, nor did they receive hormone deprivation therapy prior to the MR exam. The time between the biopsy exam and the MR exam was at least four weeks. The MRSI pulse sequence is a 3D PRESS pulse sequence with optimized 180 pulses and an echo time of 120 ms. Water and lipid signals are suppressed with two dual-frequency selective excitation pulses and crusher gradients (6). Nominal resolution of the spectroscopic voxels is 6x6x6 mm. By using a short TR (650 ms) the number of averages in the center of the elliptical, weighted acquisition scheme is maximized. The total acquisition time is between 10 and 12 minutes, depending on the exact number of phase encode steps and averages. After biopsy, the complete prostate was subject to histopathological analysis by the pathology department. The spectra from these voxels (16x16x16 for each patient) were fitted in the time domain with model functions for the three metabolite signals using the PRISMA software package. The supervised fit results include integral values (with std.dev.) for the individual metabolites and an SNR calculation of the spectrum. Treating each voxel as individual points in 3-dimensional space, where the three integrals define these dimensions, k-means clustering was applied to the data in two passes. The purpose of the first pass was to separate voxels outside the prostate from those which are inside the prostate. The remaining voxels were clustered a second time, free from the influence of the high number of outer voxels.

Results and Discussion

The final clustering results for two sample patients are shown in Figure 1. Similar processing of other patient data gave comparable results. The voxels which were identified as those residing outside the prostate form a dense cluster close to the origin and have not been displayed here. In both patients, the voxels assigned to the black and blue clusters lie on a common axis radiating outwards from the origin. Their position suggests normal prostate tissue (5). Deviating from this central branch is the red cluster. Plotting these clustering results for each slice in a 16x16 grid yields an image such as that shown in Figure 2, where the clustering results for a sample slice from the prostate of patient A are shown alongside the histopathological results of that slice. It can be seen that the red cluster corresponds to tumorous tissue, the black cluster to healthy central gland and the blue cluster to healthy peripheral zone and/or prostate edges. For patient A, a separate group of voxels can be seen close to the creatine axis. After re-assignment of this group to a new cluster, it was seen that they all exist in a region near the base of the prostate. Examination of the spectra that belong to these voxels, combined with their spatial details, suggests that these particular voxels may be overly influenced by the coil. From the histopathological reports, patient A contains large, easily delineated tumours while patient B has smaller, more scattered tumours. Some of these smaller tumours in patient B were not identified due to the low MRS resolution.

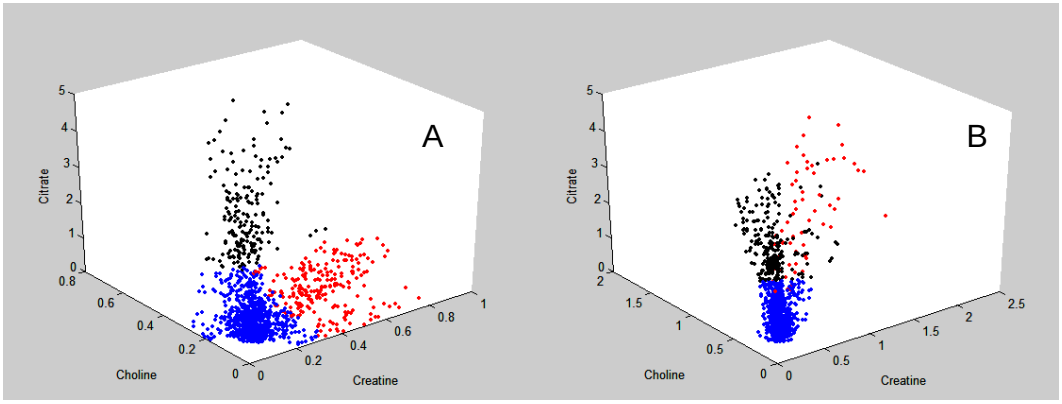

Figure 1. Results of 2-pass k-means clustering on two sample patients. Each point represents a single voxel, the colours corresponding to cluster allocation. The voxels which were found to lie outside the prostate (which lie close to the origin on these plots) have not been shown.

Conclusion

The results of this study demonstrate that unsupervised pattern recognition of MRS data of the prostate has the potential to discriminate healthy tissue from tumorous tissue, offering a useful visualisation aid for tumour localisation. The clustering results shown here are still preliminary and various clustering techniques are still being explored. One such method is mixture modelling which does not "hard"-assign voxels to classes but assigns probabilities of class membership to each voxel.

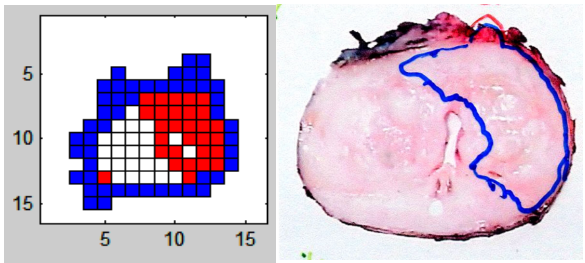

Figure 2. Prostate slice from patient A. Visualisation of slice us results of clustering analysis (left) and histopathological analy with indicated tumour region (right). Black points in Figure 1 now the white voxels (boxes) inside the prostate

References

1. Howe FA and Opstad KS. NMR Biomed 2003;16:123-131
2. Simonetti AW *et al*. Anal Chem 2003;75(20):5352-5361
3. Lukas L *et al*. Artif Intell Med 2004;31:73-89
4. http://carbon.uab.es/INTERPRET/
5. van Dorsten FA *et al*. J Magn Res Imaging 2004;20(2):279-287
6. Lack S *et al*. Magn Reson Med 1997;38:311-321